Application of antihelix antibodies in protein structure determination

Ji Won Kim[a,1], Songwon Kim[b,1], Haerim Lee[c], Geunyoung Cho[a], Sun Chang Kim[d], Hayyoung Lee[e], Mi Sun Jin[b,2], and Jie-Oh Lee[a,2]

[a]Department of Life Sciences, Pohang University of Science and Technology, Nam-gu, Pohang 37673, Korea; [b]School of Life Sciences, Gwangju Institute of Science and Technology, Buk-gu, Gwangju 61005, Korea; [c]Department of Chemistry, Korea Advanced Institute of Science and Technology, Yuseong-gu, Daejeon 34141, Korea; [d]Department of Biological Sciences, Korea Advanced Institute of Science and Technology, Yuseong-gu, Daejeon 34141, Korea; and [e]Institute of Biotechnology, Chungnam National University, Yuseong-gu, Daejeon 34134, Korea

Edited by K. C. (Chris) Christopher Garcia, Stanford University, Stanford, CA, and approved July 10, 2019 (received for review June 16, 2019)

Antibodies are indispensable tools in protein engineering and structural biology. Antibodies suitable for structural studies should recognize the 3-dimensional (3D) conformations of target proteins. Generating such antibodies and characterizing their complexes with antigens take a significant amount of time and effort. Here, we show that we can expand the application of well-characterized antibodies by "transplanting" the epitopes that they recognize to proteins with completely different structures and sequences. Previously, several antibodies have been shown to recognize the alpha-helical conformation of antigenic peptides. We demonstrate that these antibodies can be made to bind to a variety of unrelated "off-target" proteins by modifying amino acids in the preexisting alpha helices of such proteins. Using X-ray crystallography, we determined the structures of the engineered protein–antibody complexes. All of the antibodies bound to the epitope-transplanted proteins, forming accurately predictable structures. Furthermore, we showed that binding of these antihelix antibodies to the engineered target proteins can modulate their catalytic activities by trapping them in selected functional states. Our method is simple and efficient, and it will have applications in protein X-ray crystallography, electron microscopy, and nanotechnology.

X-ray crystallography | antibody | protein design

Antibody Fab or Fv fragments have been found to be useful for structural studies of challenging proteins. Currently, high-resolution structural studies of proteins by single-particle electron microscopy are limited to those with molecular masses above ∼50 kDa (1). It has been proposed that, for smaller proteins, binding of 1- or 2-antibody Fab fragments can increase the effective size of the target proteins. Antibodies can also be useful for X-ray crystallography of proteins (2, 3). They can freeze the conformation of a protein with multiple structural states into a single uniform state, and they can hide hydrophobic or flexible surfaces that interfere with crystallization. Antibodies suitable for structural studies need to recognize the 3-dimensional (3D) conformation of the target protein, because the protein–antibody complex formed must have a stable and rigid structure for effective averaging of images and for crystallization. Antibodies that bind to flexible linear regions of proteins cannot form rigid complexes and are not useful for structural analysis. However, the generation of "conformation-specific" antibodies is not straightforward for many proteins and requires special screening methods (4–6). Antibodies are essential tools in protein nanotechnology as well (7–9). Many antibodies are being used to construct complex nanostructures, because they can bind to specific components of the nanoassemblies, forming stable and predictable structures. They are also useful in functionalizing nanostructures, because antibodies can bind proteins or other molecules with useful functions. Mapping epitopes of the antibodies and characterizing structures of the antibody–antigen complexes are often the most time-consuming steps in this application, because they should be determined empirically for every antibody.

Previously, many antibodies have been shown to bind short alpha-helical peptides present in antigenic proteins. Some of these antibodies bind exclusively to a single alpha helix and have little or no interaction with other parts of a protein. For example, the 3MNZ antibody is one of numerous antibodies raised against the gp41 peptide of HIV (10). In this article, we use Protein Data Bank (PDB) ID codes to designate antibodies to avoid confusion. Gp41 is a subunit of the HIV envelope protein and forms a homotrimeric complex containing 6 alpha helices. The 3LRH intrabody is another example of an antihelix antibody (11). Intrabodies are antibodies or antibody fragments that work within the cell to bind to intracellular proteins. The 3LRH intrabody is an engineered variable domain fragment of an immunoglobulin light chain that binds to an alpha-helical stretch of 14 amino acids originating from human huntingtin protein. The binding site of the antigenic peptide is located in the concave surface formed by the beta sheet that normally interacts with the heavy-chain variable domain. When the peptide antigen binds to 3LRH intrabody, it adopts a near-ideal alpha-helical structure. The 1P4B antibody also recognizes a helical epitope with a different amino acid sequence (12). It was initially generated and selected by ribosome

Significance

Antibodies have been found to be helpful for structural studies of challenging proteins by X-ray crystallography and electron microscopy. They are being used to construct useful protein nanostructures as well. Antibodies suitable for structural study should recognize the 3-dimensional conformations of target proteins. However, generating such antibodies and characterizing structures of their complexes with antigens take months or even years of research. Here, we show that we can expand the application of well-characterized antibodies by "transplanting" the alpha-helical epitopes that they recognize to proteins with completely different structures and sequences. Systematic screening of more antihelix antibodies will greatly expand the scope of the method.

Author contributions: J.W.K., S.K., Haerim Lee, Hayyoung Lee, M.S.J., and J.-O.L. designed research; J.W.K., S.K., Haerim Lee, and G.C. performed research; J.W.K., S.K., Haerim Lee, G.C., and J.-O.L. analyzed data; and J.W.K., S.K., Haerim Lee, S.C.K., Hayyoung Lee, M.S.J., and J.-O.L. wrote the paper.

The authors declare no conflict of interest.

This article is a PNAS Direct Submission.

Data deposition: The atomic coordinates and X-ray diffraction data reported in this paper have been deposited in the Protein Data Bank (PDB) under the following ID codes: 6K68 for 8420-3MNZ, 6K65 for 9014-1P4B, 6K64 for 8188-3LRH, 6K3M for 8189-3LRH, 6K6B for 8496-3LRH, 6K67 for 9011-3LRH, 6K69 for 9213-3LRH, and 6K6A for 8188cys-3LRHcys.

See Commentary on page 17611.

[1]J.W.K. and S.K. contributed equally to this work.

[2]To whom correspondence may be addressed. Email: misunjin@gist.ac.kr or jieoh@postech.ac.kr.

This article contains supporting information online at www.pnas.org/lookup/suppl/doi:10.1073/pnas.1910080116/-/DCSupplemental.

Published online August 1, 2019.

display screening against a GCN4 peptide. The antibody binds to a 12-residue GCN4 that adopts a near-ideal alpha-helical structure when bound to the antibody.

Here, we show that helical epitopes for these antihelix antibodies can be created in a variety of off-target proteins, because most of the alpha helices found in proteins adopt a uniform backbone conformation. The resulting engineered proteins were shown to bind to the antihelix antibodies with high affinity. The formation of these complexes with predicted structures was confirmed by X-ray crystallography and negative staining electron microscopy.

Results

Creation of a 3MNZ Epitope in the C-Terminal Alpha Helix of Protein A and Determination of the Crystal Structure of the Engineered Protein A–3MNZ Single-Chain Fv Complex. The 3MNZ antibody recognizes an alpha-helical peptide with 14 amino acid residues and 2 C-terminal amino acids of gp41 (Fig. 1*A*) (10). The core interaction in the peptide–antibody complex is mediated by one side of the helix composed of hydrophobic amino acids L61, W66, and L69 and hydrophilic amino acids E62, D64, K65, and S68. The other side of the helix is fully exposed to solvent. The C-terminal N71 is not part of the helix and interacts strongly via hydrogen bonds with the heavy chain of the antibody.

The B1 domain of protein A was chosen as a test case for creating a 3MNZ epitope, because it is composed of 3 alpha helices, is readily produced in *Escherichia coli*, and can be crystallized in a variety of conditions. To engineer the protein A domain, the structure of gp41 peptide bound to the Fab fragment of the 3MNZ antibody was superimposed on that of the C-terminal helix of protein A while avoiding steric collision of antibody and protein A (*SI Appendix*, Fig. S1). Because the N-terminal 3 amino acids, from N56 to Q58, of gp41 do not interact with the antibody, the amino acids of protein A were used for the corresponding positions (Fig. 1*A*). In the docked structure, amino acids in the G44, E45, K47-L49, E51, S52, and A54 positions of protein A play key roles in antibody binding and were changed to those in the gp41 sequence (Fig. 1*B*). Amino acids V42, L43, A46, and Q53 of protein A were not changed, because they point to the hydrophobic core of protein A. The N50 position of protein A is not critical for binding; either Asn or Ala is compatible in that position, and alanine was chosen. The resulting #8420 protein A was produced in *E. coli* and purified to homogeneity. The structural integrity of the protein A does not seem to have been disturbed, because the protein can be overexpressed in *E. coli*, is highly resistant to subtilisin digestion, and elutes as a monomer in gel filtration chromatography. The engineered protein A was mixed with the purified single-chain Fv (scFv) fragment of the 3MNZ antibody, and the structure of the complex was determined by X-ray crystallography.

The crystal structure of the engineered protein A–3MNZ scFv complex shows that modification of the C-terminal helix causes practically no change in the overall structure of protein A (Fig. 1*C*), and the wild-type and engineered protein A could be superimposed with a Cα root mean square deviation (r.m.s.d.) value of 0.77 Å (*SI Appendix*, Fig. S2). The artificially created epitope adopts an alpha-helical structure as intended, and the amino acids engineered to interact with the antibody are superimposable with those of gp41 bound to 3MNZ scFv (Fig. 1*D*). These crystallographic observations prove that the epitope of 3MNZ scFv can be engineered in the C-terminal helix of protein A.

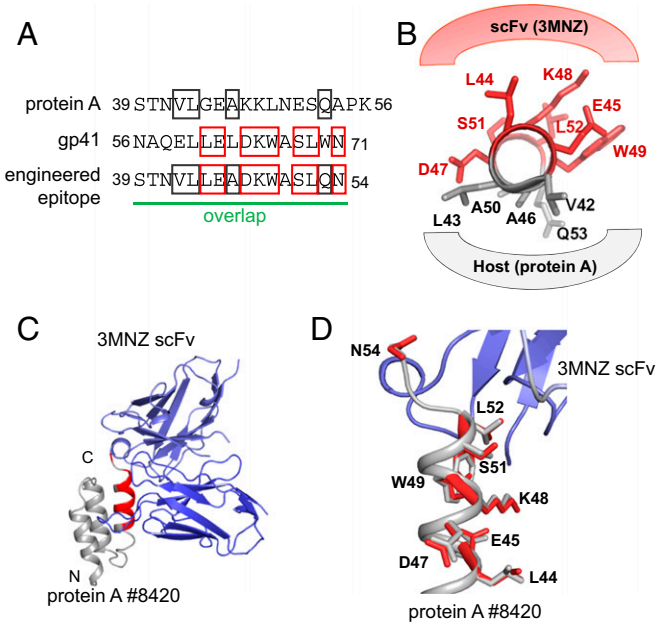

Fig. 1. Crystal structure of the 3MNZ–protein A #8420 complex. (*A*) Amino acid sequence of the engineered epitope in protein A #8420. The sequences of native protein A and the gp41 peptide are aligned after structural docking of the alpha helices (*SI Appendix*, Fig. S1). The overlap region of the docked helices is indicated by the green line. (*B*) The predicted structure of the engineered protein A with the 3MNZ epitope. The amino acid residues pointing to 3MNZ scFv and the host protein are shown in red and gray, respectively. (*C*) Crystal structure of the 3MNZ scFv and protein A #8420 complex. The amino acid residues mutated to create the epitope are in red. (*D*) Close-up view of the engineered epitope in the protein A #8420 structure. The crystal structures of protein A #8420 and the gp41 peptide bound to the 3MNZ scFv are aligned, and their amino acid residues that interact with the antibody are shown in gray and red, respectively. The view is identical to that of *C*.

Engineering of 3LRH Epitopes in the Protein A Domain. To test if other antibodies can be used as antialpha helix antibodies, we chose 3LRH intrabody for the next test, because the peptide–antibody interaction is mediated by one side of the helix and the other side is fully exposed to solvent. It is easy to produce in *E. coli* and has a high affinity for alpha-helical antigens. We created an epitope of 3LRH at 3 different positions in protein A and solved the structures of their complexes with 3LRH (Fig. 2).

The 3LRH intrabody binds to a peptide originating from human huntingtin protein. To create the epitope, the first 10 amino acids of the huntingtin peptide and the last 10 amino acids of the C-terminal helix of protein A were overlapped by a molecular modeling program (Fig. 2*A* and *SI Appendix*, Fig. S3). Amino acids K48, E51, and S52 in protein A point to the antibody and seem critical for binding (*SI Appendix*, Fig. S4). Therefore, they were changed to those of the huntingtin peptide. K48 did not need to be changed, because lysines are found in the corresponding positions of both the huntingtin peptide and the protein A sequences. The resulting #8188 protein A bound 3LRH with high affinity, and the antibody–antigen complex was purified from unbound excess proteins by gel filtration chromatography for crystallization. In the crystal structure, the modified C-terminal alpha helix of protein A interacts with the antibody as intended (Fig. 2*B* and *SI Appendix*, Fig. S5). The conformations of the amino acids interacting with the antibody were practically identical with those in the native huntingtin peptide–3LRH complex, and the overall structures of the mutant and the native proteins A could be superimposed with a Cα r.m.s.d. of 0.41 Å as planned (*SI Appendix*, Figs. S5 and S6). Introduction of a disulfide bridge enhances stability of the 3LRH complex (*SI Appendix*, Fig. S7). This may be useful for demanding nanotechnology applications, such as those encountered in animal experiments.

To prove that the epitope could be created at different positions of protein A, 2 additional epitope sites were generated in protein A (*SI Appendix*, Figs. S8 and S9). The first, #8189, was created by shifting the docking area by 1 helical turn from that of #8188 protein A. For this, an artificial C-terminal epitope was created by superimposing the 7 amino acids of the huntingtin peptide and the C-terminal helix of protein A (*SI Appendix*, Fig.

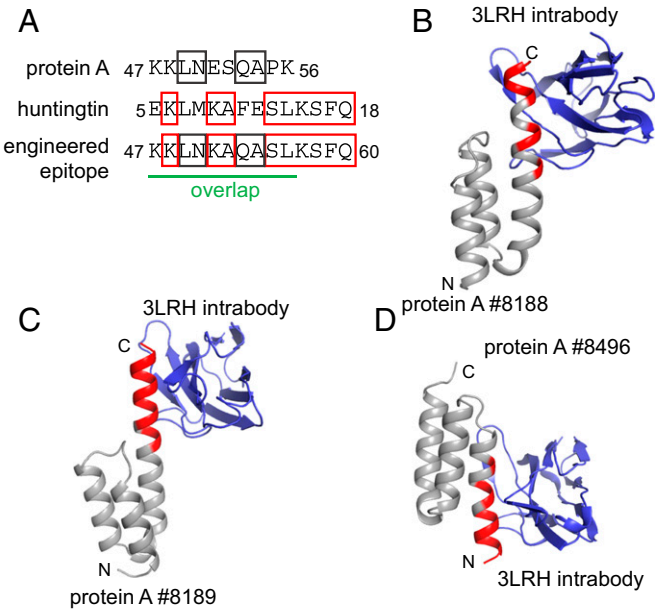

Fig. 2. Crystal structure of 3LRH–protein A complexes. (*A*) Amino acid sequence of the engineered epitope in protein A #8188. The native protein A and huntingtin sequences are aligned after structural docking of the alpha helices. The overlapped regions of the docked helices are marked with a green line. (*B*) Crystal structure of the 3LRH intrabody and protein A #8188 complex. The amino acid residues mutated to create the epitope are in red. (*C*) Crystal structure of the 3LRH intrabody and protein A #8189 complex. The amino acid residues mutated to create the epitope are in red. (*D*) Crystal structure of the 3LRH intrabody and protein A #8496 complex.

S8). The amino acids in the protein A structure pointing to the 3LRH intrabody were changed to those of the huntingtin peptide, and the amino acids pointing to the core of protein A were not changed. The second epitope was generated by mutating the N-terminal helix of protein A using a similar strategy (*SI Appendix*, Fig. S9). As intended, the 2 mutant proteins formed stable complexes with 3LRH intrabody, the complexes were not dissociated by gel filtration chromatography, and their structures could be determined. The crystal structures showed that the amino acids mutated to create the epitopes interacted with the antibody as planned, and their structures were superimposable on the designed structures (Fig. 2 *C* and *D* and *SI Appendix*, Fig. S10).

Engineering of the 3LRH Epitope in Calmodulin. To test if artificial helical epitopes could be created in proteins other than protein A, the 3LRH epitope was engineered in the N-terminal helix of calmodulin (Fig. 3*A* and *SI Appendix*, Fig. S11). Calmodulin is a calcium sensor and binds to calcium ions via EF hand motifs (13). It is composed of N- and C-terminal domains that are homologous in sequence as well as in structure. Each domain contains 2 calcium binding EF hand motifs. To generate the 3LRH epitope, the N-terminal helix of the N-terminal domain of calmodulin was docked with the huntingtin peptide by overlapping the first 8 amino acids of the calmodulin helix and the last 8 amino acids of the huntingtin helix (Fig. 3*A*). As with protein A, the amino acids pointing to the solvent in the overlapped region were changed to those of the huntingtin peptide (*SI Appendix*, Fig. S11). The resulting mutant N-terminal fragment of calmodulin binds strongly to 3LRH intrabody, and the complex can be crystallized. As designed, the structure of the calmodulin part of the calmodulin–3LRH complex is not changed with the exception of the last 3 amino acids, the structure of which appears unstable in the absence of the C-terminal calmodulin fragment (*SI Appendix*, Fig. S12*A*). The 2 calcium binding sites of the engineered calmodulin fragment are occupied by calcium ions, demonstrating that the functional and structural integrity of the protein is not disturbed (Fig. 3*B*). The overall structure of the engineered 3LRH epitope is superimposable with that of the huntingtin peptide in the 3LRH complex, proving the success of the design (Fig. 3*B* and *SI Appendix*, Fig. S12*B*).

Engineering of the 3LRH Epitope in an Internal Alpha Helix. To show that helical epitopes can be created in internal helices as well as in terminal helices, we engineered a 3LRH epitope in an internal helix of T4 lysozyme. The lysozyme is composed of 11 alpha helices and 3 short beta strands, and we created the 3LRH epitope in the second alpha helix (Fig. 3*C* and *SI Appendix*, Fig. S13). To connect the third beta strand and the engineered second alpha helix, which is extended by 3 additional helical turns, we inserted a linker with 12 flexible amino acids (Fig. 3*D* and *SI Appendix*, Table S1). The mutated lysozyme protein was produced in *E. coli* and crystallized as a complex with 3LRH intrabody. The crystal structure confirms that the 3LRH epitope has been created and that the mutated lysozyme binds to the antibody (Fig. 3*D*). The side chains interacting with the antibody in the 3LRH complex have practically identical conformations to those in the huntingtin peptide (*SI Appendix*, Fig. S14).

Engineering of the 1P4B Epitope in a Protein A Domain and Crystal Structure of the Protein A–1P4B scFv Complex. As the last test case, we chose the 1P4B antibody because of its high affinity for the alpha-helical antigen of GCN4 and its efficient expression in *E. coli*. The peptide–antibody interaction of the 1P4B antibody is again mediated by one side of the helix, and the other side is fully exposed to solvent. As in the other cases, we docked the 1P4B–GCN4 structure to the C-terminal helix of the protein A domain while avoiding steric collision of protein A and antibody. Then, the amino acid residues interacting with the antibody were mutated to those of the GCN4 peptide (Fig. 4*A* and *SI Appendix*, Fig. S15). Protein A and the scFv fragment of 1P4B formed a

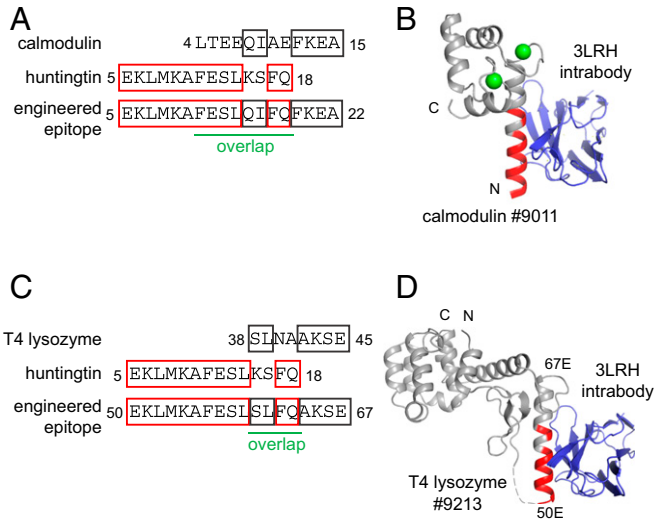

Fig. 3. Crystal structure of the 3LRH–calmodulin and the 3LRH–T4 lysozyme complexes. (*A*) Amino acid sequence of the engineered epitope in calmodulin #9011. The native calmodulin and huntingtin sequences are aligned after structural docking of the alpha helices. The overlapped region of the docked helices is marked with a green line. (*B*) Crystal structure of the 3LRH intrabody and calmodulin #9011 complex. The amino acid residues mutated to create the epitope are in red. The calcium ions bound to the calmodulin are drawn as green balls. (*C*) Amino acid sequence of the engineered epitope in lysozyme #9213. The native lysozyme and huntingtin sequences are aligned after structural docking of the alpha helices. The overlapped regions of the docked helices are marked with a green line. (*D*) Crystal structure of the 3LRH intrabody and lysozyme #9213 complex. The amino acid residues mutated to create the epitope are colored in red. The flexible "VEGGGGSGGGGS" linker is not visible in the electron density map and is marked with a broken gray line.

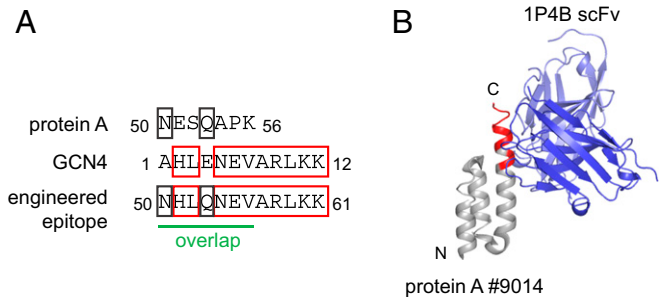

Fig. 4. Crystal structure of the 1P4B–protein A #9014 complex. (*A*) Amino acid sequence of the engineered epitope in the protein A #9014. The native protein A and the GCN4 sequences are aligned after structural docking of the alpha helices. The overlapped regions of the docked helices are marked with a green line. (*B*) Crystal structure of the 1P4B scFv and protein A #9014 complex. The amino acid residues mutated to create the epitope are colored in red.

stable complex, and the purified complex was crystallized for structural analysis. The mutated protein A, #9014, binds to the antibody fragment, forming the intended structure, and the amino acids mutated to bind to the antibody fragment adopt practically identical conformations to those of the GCN4 peptide in the 1P4B complex (Fig. 4*B* and *SI Appendix*, Figs. S16 and S17).

Engineering of the 1P4B Epitope in the ABCB6 Transporter. We tested if our antihelix antibodies are useful for study of membrane proteins with unknown structures. Human ABCB6 was chosen as the target protein. ABCB6 is a mitochondrial Adenosine triphosphate (ATP) binding cassette (ABC) transporter that regulates heme and porphyrin synthesis by translocating coproporphyrinogen III from the cytoplasm into mitochondria (14). The monomeric ABCB6 is a half transporter, containing 1 transmembrane domain (TMD) and 1 nucleotide binding domain (NBD) that becomes active by forming a homodimer. Crystal structure of the isolated NBD has been determined (15). However, the structure of ABCB6 containing TMD has not been reported yet. Therefore, we predicted its structure using a homology modeling technique. Structure of Atm1-type ABC exporter (NaAtm1; PDB ID code 4MRS) that has 46% homology in sequence with human ABCB6 was used as the template, and the program MODELER was used for calculation (16, 17). We observed that the homology model of the NBD closely matches the crystal structure, demonstrating accuracy of the modeling (*SI Appendix*, Fig. S18) (15). The NBD of ABCB6 contains a short helix at its C terminus (*SI Appendix*, Fig. S18*B*). To transplant the 1P4B epitope onto it, the C-terminal helix of the NBD domain of ABCB6 was docked with the GCN4 peptide by overlapping the last 3 amino acids of ABCB6 and the first 3 amino acids of the GCN4 helix (*SI Appendix*, Fig. S19). The amino acids exposed to the solvent in the overlap region were again changed to those of GCN4 peptide, while the amino acids pointing to ABCB6 were not changed. Q823 of ABCB6 is not in the overlap region but appeared to collide with the W109 and S111 residues of 1P4B scFv in the docking model (*SI Appendix*, Fig. S20). Therefore, the glutamine was changed to alanine (Q823A) to avoid this collision.

To facilitate visualization of ABCB6 in the micrographs, we introduced 2 mutations. First, we truncated the lysosomal targeting segment of human ABCB6, residues 1 to 205, to improve the homogeneity of the protein as shown previously (18). Second, we also introduced an E659Q mutation into the NBD domain of ABCB6 to disrupt ATP hydrolysis activity and stabilize the outward-facing structure (19–23). The engineered ABCB6 was produced in *Pichia pastoris*, and purified ABCB6 was incubated with 1P4B Fab at a molar ratio of 1:3 to form stable complexes. The complexes and excess antibody were separated by size exclusion chromatography (Fig. 5 *A* and *B*). The pooled fractions containing the ABCB6–Fab complex were then mixed with ATP/Mg^{2+} to trap ABCB6 in the ATP-bound, outward-facing catalytic state. The resulting protein complex was subjected to negative staining electron microscopy (EM) and single-particle analysis. In total, 153,945 and 138,419 particles were collected and used to obtain 2-dimensional (2D) class averages of ABCB6 with and without bound 1P4B Fab, respectively. The major 2D class averages of ABCB6 without the bound antibody exhibited the characteristic structural features of ABC transporters: the TMDs embedded in the detergent micelles and the NBDs forming a closed dimer. By contrast, the EM images of the ABCB6–1P4B Fab complex clearly included extra densities corresponding to dumbbell-shaped Fab bound to the presumed NBD binding site (Fig. 5 *C* and *D*). The 3D reconstructions confirmed that the location of the Fab density was in agreement with the designed structure, thus showing that the protein with artificially designed epitope adopted the intended structure (Fig. 5 *E* and *F*). Because of the flexibility between the variable and constant regions of Fab, only the Fv region is seen in the final density map.

In our structure, only 1 molecule of Fab is bound to 1 NBD domain, because steric hindrance prevents binding to the other domain as predicted. During purification, cholesteryl hemisuccinate was added to the detergent to stabilize the structure of ABCB6 and maintain its activity, and this may be responsible for the slightly larger dimensions of the detergent micelles (Fig. 5 *E* and *F*) (24). Because the resolution of our EM maps was not sufficient to build a model for ABCB6 directly, we fitted the known structure of a bacterial homolog of P-glycoprotein (P-gp),

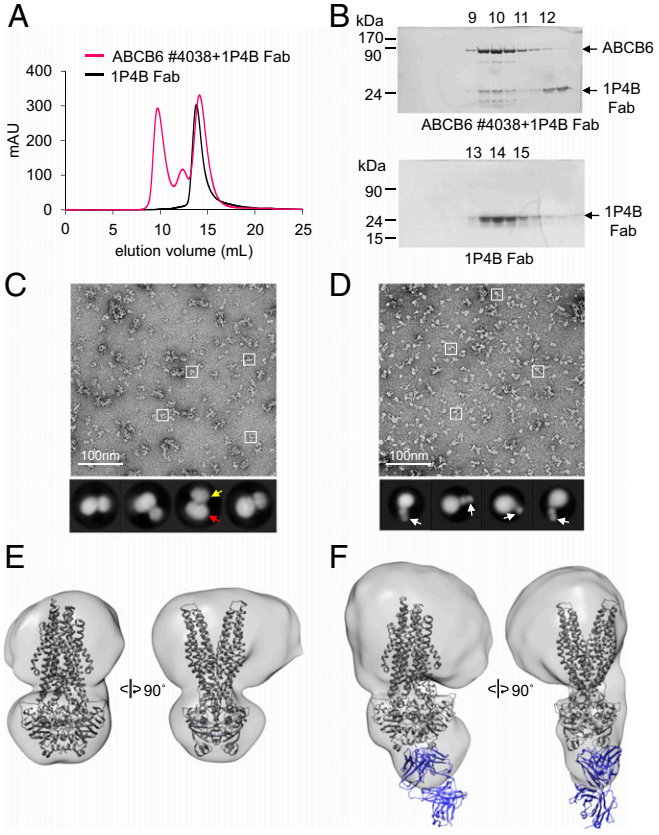

Fig. 5. The interaction between human ABCB6 and the 1P4B Fab. (*A*) Size exclusion chromatography profiles and (*B*) SDS-PAGE analysis of the ABCB6–1P4B Fab complex. The ABCB6 and 1P4B Fab bands are indicated by black arrows. (*C* and *D*) EM micrographs of ABCB6 with and without the 1P4B Fab. A few representative particles are boxed, and major 2D average classes are shown underneath. The red, yellow, and white arrows indicate detergent micelles, the cytosolic NBD domain, and 1P4B Fab bound to ABCB6, respectively. (*E* and *F*) EM maps with the docked crystal structure of a bacterial multidrug ABC transporter, Sav1866, with PDB ID code 2ONJ in the outward-facing conformation.

Sav1866 from *Staphylococcus aureus*, to the final density map (14). Our EM maps closely match the Sav1866 structure, indicating that ABCB6 has an outward-facing TMD (i.e., open to the mitochondrial intermembrane space) and a closed NBD conformation. High-resolution cryo-EM study of the ABCB6–1P4B complex is underway.

Engineering of the 1P4B and 3LRH Epitopes in P-gp and Inhibition of Its ATP Hydrolysis Activity. To test if the antihelix antibodies can be used to stabilize specific conformational states of proteins, we chose *Caenorhabditis elegans* P-gp as a model protein (25). P-gp, a member of the ABC transporter superfamily, is a major multidrug transporter that can confer drug resistance by pumping anticancer drugs out of cancer cells. The functional unit of P-gp is composed of homologous N-terminal and C-terminal halves, each containing a TMD (TMD1 and TMD2) and a cytoplasmic NBD (NBD1 and NBD2) in a single polypeptide (Fig. 6 *A* and *B*). The TMDs recognize various substrates and facilitate their translocation across the membrane, while the NBDs bind and hydrolyze ATP, providing the energy for substrate translocation.

To introduce a 1P4B epitope into P-gp, a short helix at the C terminus of NBD1 was docked with the GCN4 peptide by overlapping the last 12 amino acids of the NBD1 helix and the first 12 amino acids of the GCN4 peptide (Fig. 6*A* and *SI Appendix*, Fig. S21 *A* and *B*). The amino acids of the NBD1 helix exposed to solvent were substituted for those of the GCN4 peptide, while the amino acids pointing toward the center of NBD1 were not. Using a similar strategy, the 3LRH epitope was also created on the P-gp NBD1, but its docking area was shifted by 1 helical turn from that of 1P4B to avoid steric collision with the host protein (Fig. 6*B* and *SI Appendix*, Fig. S21 *C* and *D*).

To verify the interactions of the engineered P-gps with antibodies in vitro, pull-down assays were performed. For this, the engineered P-gps with eGFP and decahistidine tags at their C termini were bound to nickel-nitrilotriacetic acid (Ni-NTA) resin and incubated with 1P4B scFv or 3LRH intrabody in molar ratios of 1:10. After thorough washing, the protein mixtures were separated on sodium dodecyl sulfate (SDS)-polyacrylamide gel electrophoresis (PAGE) gels. Wild-type P-gp was used as the first negative control, and empty resin without bound P-gp was used as the second negative control to exclude the possibility of background binding. Our results revealed that the engineered P-gps interacted strongly with both antibodies (*SI Appendix*, Fig. S22). The formation of stable complexes was confirmed by size exclusion chromatography as well: both antibodies eluted in the high-molecular mass fraction typical of complexes stabilized by strong interactions (*SI Appendix*, Fig. S23).

It has been demonstrated that the formation of a closed NBD dimer is a prerequisite for the ATPase activity of ABC transporters (23, 26). Our structure-based docking models suggest that binding of antihelix antibodies to the engineered P-gp inhibits its ATP hydrolysis activity by sterically preventing the closing motion of the NBD domains. To confirm this idea, we measured the ATPase activity of the purified P-gp in the presence and absence of antibodies using the potent anticancer drugs, Paclitaxel and Actinomycin D, as drug substrates. As expected for an ABC transporter, all of the P-gp structures without antibodies displayed drug-stimulated ATPase activities, and engineering of the P-gp had almost no effect on its enzymatic characteristics, such as drug concentration dependence, maximum level of stimulation by drugs, and biphasic responses to substrates, with low concentrations stimulatory and high concentrations inhibitory (Fig. 6 *C* and *D*). This strongly suggests that transplanting helix epitopes to the host proteins did not affect their intrinsic function or damage their overall structures. However, both the 1P4B scFv and the 3LRH intrabody inhibited the basal and drug-stimulated ATPase activities of the engineered P-gps (Fig. 6 *C* and *D*). This demonstrates that binding of antihelix antibodies to the engineered P-gps inhibited the structural switching of the protein to the closed state that is essential for ATPase activity. This is highly reminiscent of the effect of binding of nanobody to mouse P-gp NBD1 on its ATPase activity (27).

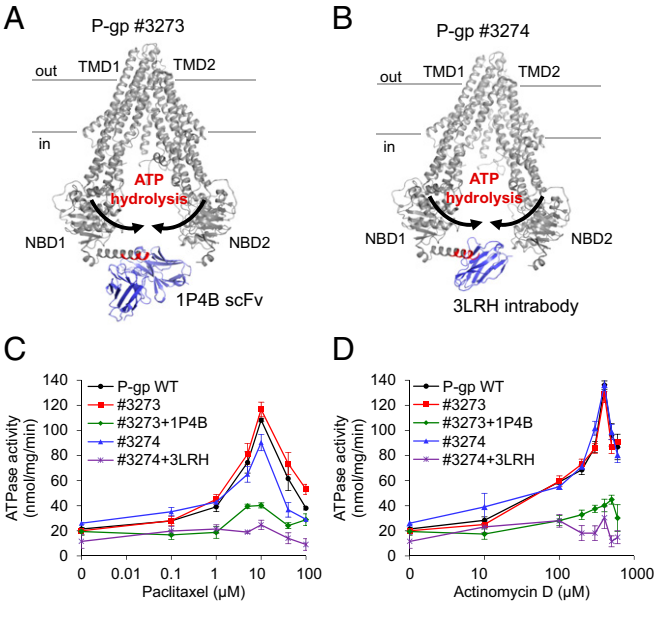

Fig. 6. Engineering of the 1P4B or 3LRH epitopes into the *C. elegans* P-gp. (*A*) The predicted structure of the 1P4B scFv and P-gp #3273 complexes. Closing motion of the NBD induced by ATP hydrolysis is prohibited by the bound antibody. The amino acid residues changed to create the 1P4B epitope are in red. (*B*) The predicted structure of the 3LRH intrabody and P-gp #3274 complex. The amino acid residues changed to create the 3LRH epitope are in red. (*C* and *D*) ATPase activity in the presence and absence of antibody. Drug-stimulated ATPase activities were measured with (*C*) paclitaxel and (*D*) actinomycin D. Data points indicate the average activities from 3 separate experiments. Error bars indicate ±SDs. WT, wild type.

Discussion

We have shown that several antibodies against alpha helices can be made to bind diverse unrelated proteins by mutating solvent-exposed amino acids in the alpha helix to those that can interact with the antibodies. The residues important for structural stability of the alpha helix are not changed in order to not disrupt the native structures of the host proteins. We have shown that our method is valid by determining the structures of 8 engineered protein–antibody complexes by X-ray crystallography. In all cases, the overall structure of each mutated protein is not seriously disturbed, and the mutated helix interacts with the antihelix antibodies as intended. Moreover, the amino acids directly interacting with the antibody adopt conformations that are identical to those found in the native peptide–antibody complexes.

Our antihelix method can be used in the following situations. First, if there is structural information on paralog or ortholog proteins, the method can be used to design epitopes in the target proteins by homology modeling. Second, it can be used when the structure of part of a protein complex is known. For example, if the structure of a ligand protein is known, it can be used to design epitopes in the ligand protein part of a ligand–receptor complex with structure that is unknown. Third, our method could be particularly useful in structural studies of transmembrane proteins, because most of them are composed entirely of long alpha helices. Antibody Fab fragments have been successfully used in structural analysis of transmembrane proteins (4, 5). However, the production of high-affinity antibodies against transmembrane proteins with small hydrophilic areas takes significant amount of time and effort. Fourth, in drug design experiments, one needs to determine the structures of hundreds of protein–drug complexes in a high-throughput fashion, and the bound antibody may be helpful for identifying crystallization or cryo-EM conditions

more convenient for high-throughput use. As with many other protein engineering methods being used in structural biology, the application of our antihelix antibody approach needs careful control experiments to show that the functional and structural integrity of the host protein has not been compromised by mutations introduced into the helix.

To test the validity of our method, we used 3 antibody fragments (3MNZ, 3LRH, and 1P4B) that have been previously shown to bind alpha-helical peptides. All of the antibodies bound to the engineered proteins, forming the expected rigid structures. This success suggests that many other helix binding antibodies could be applied in our antihelix antibody method. Thousands of antibody–antigen structures have already been deposited in the PDB. A quick survey of these structures showed that more than 10 antibodies could be used as antihelix antibodies. Moreover, since these antibodies were generated for other purposes, the antihelix antibody pool could be drastically increased if a more systematic method of generating and screening antibodies for use in our antihelix antibody method was attempted. To apply our antihelix method, the target alpha helices should be well exposed to the solvent, because steric collision of the antibodies and target proteins would interfere with binding. Having a panel of antibodies with different sequences and structures would be useful, because different antibodies recognize different structures, and at least 1 antibody that did not produce steric collision might well be present among a panel of candidate antihelix antibodies.

In conclusion, we have shown that several antibodies reported to bind to alpha helices can be used as semiuniversal antihelix antibodies. These antibodies will be convenient tools in the structural study of proteins by X-ray crystallography and cryo-EM. They can also be used to assemble protein subunits with predictable structures for protein nanotechnology. Systematic screening of more antihelix antibodies should greatly expand the scope of the method.

Materials and Methods

Preparation of the Antibody-Engineered Protein Complexes. To make the 3MNZ scFv–protein A #8420 complex, the purified antibody fragment and engineered protein were mixed in a 1:1 molar ratio for 1 h at 4 °C. Complex formation was monitored by native PAGE. Other antibody–protein complexes were purified after mixing by Superdex 200 gel filtration chromatography to remove unbound protein. The antibody–protein complexes were concentrated to 5 mg/mL before crystallization.

Crystallization and Data Collection. The crystallization conditions for the antibody-engineered protein complexes and freezing conditions for their crystals are summarized in *SI Appendix*, Table S2. All crystals were flash frozen in liquid nitrogen at −170 °C. Diffraction data were collected at the 7A and 5C beam lines of the Pohang Accelerator Laboratory. The package HKL2000 was used to index, integrate, and scale the diffraction data (HKL Research).

Structure Determination, Refinement, and Homology Modeling. Initial phases were calculated by the molecular replacement technique using the program PHASER (28). Atomic models were built by iterative modeling and refinement using the programs COOT and PHENIX (29, 30). Crystallographic data are summarized in *SI Appendix*, Tables S3 and S4. The homology model of human ABCB6 without the lysosomal targeting segment (residues 1 to 205) was generated by the program MODELER (https://salilab.org/modeller/) based on the structure of Atm1-type ABC exporter from *Novosphingobium aromaticivorans* DSM 12444, NaAtm1 (16, 17). Protocols for preparation of antibodies, preparation of engineered proteins, ATP hydrolysis activity, preparation of samples for negative EM and image acquisition, and EM data processing and image analysis are described in *SI Appendix*. Atomic coordinates and diffraction data have been deposited in the PDB (*SI Appendix*, Tables S2 and S3).

ACKNOWLEDGMENTS. We thank the staff of the beam lines 5C and 7A, Pohang Accelerator Laboratory for help with data collection and Dr. Julian Gross for critical reading of the manuscript. This research was supported by National Research Foundation Grants NRF 2017R1A2A1A17069497 and NRF-2017M3A9F6029753 funded by the Ministry of Science and ICT of Korea and Samsung Science and Technology Foundation Grant SSTF-BA1702-14.

1. A. Merk *et al.*, Breaking cryo-EM resolution barriers to facilitate drug discovery. *Cell* **165**, 1698–1707 (2016).
2. S. Koide, Engineering of recombinant crystallization chaperones. *Curr. Opin. Struct. Biol.* **19**, 449–457 (2009).
3. A. K. Shukla, C. Gupta, A. Srivastava, D. Jaiman, Antibody fragments for stabilization and crystallization of G protein-coupled receptors and their signaling complexes. *Methods Enzymol.* **557**, 247–258 (2015).
4. A. K. Shukla *et al.*, Structure of active β-arrestin-1 bound to a G-protein-coupled receptor phosphopeptide. *Nature* **497**, 137–141 (2013).
5. A. K. Shukla, G. Singh, E. Ghosh, Emerging structural insights into biased GPCR signaling. *Trends Biochem. Sci.* **39**, 594–602 (2014).
6. C. Hunte, H. Michel, Crystallisation of membrane proteins mediated by antibody fragments. *Curr. Opin. Struct. Biol.* **12**, 503–508 (2002).
7. Y. S. Chen, M. Y. Hong, G. S. Huang, A protein transistor made of an antibody molecule and two gold nanoparticles. *Nat. Nanotechnol.* **7**, 197–203 (2012).
8. J. L. Corchero, E. Vázquez, E. García-Fruitós, N. Ferrer-Miralles, A. Villaverde, Recombinant protein materials for bioengineering and nanomedicine. *Nanomedicine* **9**, 2817–2828 (2014).
9. A. Makaraviciute, A. Ramanaviciene, Site-directed antibody immobilization techniques for immunosensors. *Biosens. Bioelectron.* **50**, 460–471 (2013).
10. N. I. Nicely *et al.*, Crystal structure of a non-neutralizing antibody to the HIV-1 gp41 membrane-proximal external region. *Nat. Struct. Mol. Biol.* **17**, 1492–1494 (2010).
11. A. Schiefner *et al.*, A disulfide-free single-domain V(L) intrabody with blocking activity towards huntingtin reveals a novel mode of epitope recognition. *J. Mol. Biol.* **414**, 337–355 (2011).
12. C. Zahnd *et al.*, Directed in vitro evolution and crystallographic analysis of a peptide-binding single chain antibody fragment (scFv) with low picomolar affinity. *J. Biol. Chem.* **279**, 18870–18877 (2004).
13. W. E. Meador, A. R. Means, F. A. Quiocho, Target enzyme recognition by calmodulin: 2.4 A structure of a calmodulin-peptide complex. *Science* **257**, 1251–1255 (1992).
14. R. J. Dawson, K. P. Locher, Structure of a bacterial multidrug ABC transporter. *Nature* **443**, 180–185 (2006).
15. M. Haffke, A. Menzel, Y. Carius, D. Jahn, D. W. Heinz, Structures of the nucleotide-binding domain of the human ABCB6 transporter and its complexes with nucleotides. *Acta Crystallogr. D Biol. Crystallogr.* **66**, 979–987 (2010).
16. B. Webb, A. Sali, Protein structure modeling with MODELLER. *Methods Mol. Biol.* **1654**, 39–54 (2017).
17. J. Y. Lee, J. G. Yang, D. Zhitnitsky, O. Lewinson, D. C. Rees, Structural basis for heavy metal detoxification by an Atm1-type ABC exporter. *Science* **343**, 1133–1136 (2014).
18. K. Kiss *et al.*, Role of the N-terminal transmembrane domain in the endo-lysosomal targeting and function of the human ABCB6 protein. *Biochem. J.* **467**, 127–139 (2015).
19. J. Zaitseva, S. Jenewein, T. Jumpertz, I. B. Holland, L. Schmitt, H662 is the linchpin of ATP hydrolysis in the nucleotide-binding domain of the ABC transporter HlyB. *EMBO J.* **24**, 1901–1910 (2005).
20. J. Zaitseva *et al.*, A structural analysis of asymmetry required for catalytic activity of an ABC-ATPase domain dimer. *EMBO J.* **25**, 3432–3443 (2006).
21. J. E. Moody, L. Millen, D. Binns, J. F. Hunt, P. J. Thomas, Cooperative, ATP-dependent association of the nucleotide binding cassettes during the catalytic cycle of ATP-binding cassette transporters. *J. Biol. Chem.* **277**, 21111–21114 (2002).
22. C. Orelle, O. Dalmas, P. Gros, A. Di Pietro, J. M. Jault, The conserved glutamate residue adjacent to the Walker-B motif is the catalytic base for ATP hydrolysis in the ATP-binding cassette transporter BmrA. *J. Biol. Chem.* **278**, 47002–47008 (2003).
23. M. L. Oldham, D. Khare, F. A. Quiocho, A. L. Davidson, J. Chen, Crystal structure of a catalytic intermediate of the maltose transporter. *Nature* **450**, 515–521 (2007).
24. A. A. Thompson *et al.*, GPCR stabilization using the bicelle-like architecture of mixed sterol-detergent micelles. *Methods* **55**, 310–317 (2011).
25. M. S. Jin, M. L. Oldham, Q. Zhang, J. Chen, Crystal structure of the multidrug transporter P-glycoprotein from Caenorhabditis elegans. *Nature* **490**, 566–569 (2012).
26. P. C. Krishnamurthy *et al.*, Identification of a mammalian mitochondrial porphyrin transporter. *Nature* **443**, 586–589 (2006).
27. A. B. Ward *et al.*, Structures of P-glycoprotein reveal its conformational flexibility and an epitope on the nucleotide-binding domain. *Proc. Natl. Acad. Sci. U.S.A.* **110**, 13386–13391 (2013).
28. A. J. McCoy *et al.*, Phaser crystallographic software. *J. Appl. Crystallogr.* **40**, 658–674 (2007).
29. P. D. Adams *et al.*, PHENIX: A comprehensive Python-based system for macromolecular structure solution. *Acta Crystallogr. D Biol. Crystallogr.* **66**, 213–221 (2010).
30. P. Emsley, B. Lohkamp, W. G. Scott, K. Cowtan, Features and development of Coot. *Acta Crystallogr. D Biol. Crystallogr.* **66**, 486–501 (2010).